UDC 621.314 https://doi.org/10.20998/2074-272X.2026.3.05

R.F. Abdelgoui, R. Taleb

Enhanced power quality in grid-connected wind energy systems using PI-controlled with doubly fed induction generator optimized by hybrid differential evolution and grey wolf algorithm

Introduction. *Nowadays, the most widely used wind energy conversion system in wind farms is based on a doubly fed induction generator (DFIG); it has a large speed range and can function in multiple modes.* ***Problem.*** *Harmonic distortion in wind energy conversion system can degrade output waveform quality, reduce power conversion efficiency.* ***Goal.*** *This study investigates the dynamic performance of a wind energy conversion system comprising a grid-connected load, a 13-level hybrid multilevel converter and a doubly fed induction generator (DFIG), using a PI controller. The study aims to evaluate the dynamic performance and power quality of wind energy conversion systems, and to develop a novel hybrid metaheuristic method combining differential evolution (DE) and grey wolf optimization (GWO)-based selective harmonic elimination pulse-width modulation (SHEPWM) control strategies. This method reduces total harmonic distortion (THD) and ensures compliance with IEEE 519 standards, while increasing the power transferred to the grid.* ***Methodology.*** *The system, which includes a grid-connected load, a 13-level converter, and a DFIG, is modeled and simulated in MATLAB/Simulink under steady-state wind conditions. Vector control via stator flow orientation was used to modify the energy quality provided by the DFIG, making the system comparable to the DC machine. Our approach was to use a PI controller in order to directly control the active and reactive DFIG power through multi-level converter then a hybrid metaheuristic algorithm combining DE and GWO is implemented to solve the SHEPWM nonlinear transcendental equations. The proposed algorithm is evaluated based on its ability to suppress lower-order harmonics and improve THD performance, these converters increase the power transmitted to the power grid by reducing harmonic content of the output voltages.* ***Results.*** *By using the DE-GWO hybrid method and a PI controller, lower-order harmonics were effectively removed and THD was reduced to meet IEEE 519 standards. Simulations showed an improvement in output wave quality and better energy conversion efficiency compared to conventional optimization methods.* ***Scientific novelty*** *of the proposed work lies in the fact that the study introduces a novel DE-GWO hybrid optimization method for PWM (SHEPWM) in 13-level hybrid multilevel converter applied to wind energy systems.* ***Practical value.*** *The novel method demonstrates that constant high performance in wind energy systems may be achieved by combining intelligent optimization algorithms with complex multilevel converter designs This means it can be effectively integrated into contemporary wind farms where meeting grid standards, adjusting to varying sizes, and ensuring long-term reliability are crucial.* References 26, table 1, figures 19.

Key words: **doubly fed induction generator, wind power, differential evolution, power quality, total harmonic distortion.**

Вступ. *На сьогодні найбільш поширеною системою перетворення енергії вітру у вітрових електростанціях є система на основі асинхронного генератора з подвійним живленням (DFIG); вона характеризується широким діапазоном швидкостей і здатністю працювати в різних режимах.* ***Проблема***. *Гармонічні спотворення в системах перетворення вітрової енергії можуть погіршувати якість вихідної напруги та знижувати ефективність перетворення енергії.* ***Мета***. *У роботі розглядається динамічна поведінка системи перетворення вітрової енергії, що включає навантаження, підключене до мережі, 13-рівневий гібридний багаторівневий перетворювач та асинхронний генератор з подвійним живленням (DFIG), із застосуванням ПІ-регулятора. Метою роботи є оцінка динамічних характеристик і якості електроенергії, а також розроблення нового гібридного метаевристичного методу, що поєднує диференціальну еволюцію (DE) та оптимізацію сірого вовка (GWO) для керування за методом селективного усунення гармонік із широтно-імпульсною модуляцією (SHEPWM). Запропонований метод забезпечує зменшення коефіцієнта гармонічних спотворень (THD), відповідність стандарту IEEE 519 та підвищення потужності, що передається до мережі.* ***Методика***. *Система, що включає навантаження, підключене до мережі, 13-рівневий перетворювач і DFIG, змодельована та досліджена в середовищі MATLAB/Simulink за усталених умов вітру. Для покращення якості електроенергії використано векторне керування з орієнтацією за потоком статора, що забезпечує характеристики, подібні до машин постійного струму. Активна та реактивна потужності DFIG безпосередньо регулюються за допомогою ПІ-регулятора через багаторівневий перетворювач. Для розв'язання нелінійних трансцендентних рівнянь SHEPWM застосовано гібридний метаевристичний алгоритм, що поєднує DE та GWO. Ефективність алгоритму оцінюється за здатністю пригнічувати гармоніки нижчих порядків та зменшувати THD. Використання багаторівневих перетворювачів сприяє збільшенню переданої до мережі потужності за рахунок зниження гармонічних спотворень вихідної напруги.* ***Результати***. *Застосування гібридного методу DE-GWO у поєднанні з ПІ-регулятором забезпечило ефективне придушення гармонік нижчих порядків і зниження THD до рівня, що відповідає вимогам стандарту IEEE 519. Результати моделювання показали покращення якості вихідної напруги та підвищення ефективності перетворення енергії порівняно з традиційними методами оптимізації.* ***Наукова новизна*** *полягає у розробленні нового гібридного методу оптимізації DE-GWO для широтно-імпульсної модуляції типу SHEPWM у 13-рівневому гібридному багаторівневому перетворювачі, застосованому в системах вітроенергетики.* ***Практична значимість***. *Запропонований метод демонструє можливість досягнення стабільно високих показників роботи систем вітроенергетики шляхом поєднання інтелектуальних алгоритмів оптимізації зі складними багаторівневими перетворювачами. Це забезпечує ефективну інтеграцію в сучасні вітрові електростанції, де критично важливими є відповідність мережевим стандартам, адаптивність до змін умов роботи та довготривала надійність.* Бібл. 26, табл. 1, рис. 19.

Ключові слова: **асинхронний генератор з подвійним живленням, вітроенергетика, диференціальна еволюція, якість електроенергії, коефіцієнт гармонічних спотворень.**

Introduction. One of the most efficient power generation systems is wind power. However, in the case of grid-connected structures, different electrical generators can be used. The doubly fed induction generator (DFIG) is still widely used capacitors for reactive power compensation [1]. In addition, the main advantage of this generator is the power converters, which are smaller than traditional full-size stator converters. Several techniques have been proposed in the literature to develop appropriate, economical and effective wind energy conversion systems for microgrid connection [2, 3].

Wind power is crucial to the electrical grid, thus cutting it off during a breakdown can cause instability and exacerbate the voltage surge. Because of this, the new grid standards have established stringent guidelines for how wind producers must behave in these circumstances. Depending on the severity of the fault, fault ride-through criteria include power delivery, an uninterrupted connection, and a contribution to grid stability for a specific amount of time [4]. Several solutions have been

proposed in the literature to meet the requirements of the grid code while ensuring the reliable and safe operation of the DFIG [5, 6].Converter based multi-level architectures improve load power efficiency. Compared to standard 2-level inverters that require a high switching frequency, multi-level converters offer advantages. Because of its high efficiency, significant voltage operating capacity, low output of electromagnetic interference, and reduced switching losses, multi-level inverters are gaining increased attention from academics. In addition to minimizing the stress of d*v*/d*t*, multi-level converters can give incredibly low voltage distortion, which lessens electromagnetic compatibility issues. Both fundamental frequencies and high PWM switching frequencies can be utilized with them [7, 8].

Space-vector pulse-width modulation (PWM) gating of the inverter switches enhances the fundamental alone at the alternating current sides as well as the utilization of the available voltage [4]. Selective harmonic elimination (SHEPWM), on the other hand, is typically a better option when only specific low-order harmonics need to be cancelled. This type of PWM produces ideal switching angles that satisfy a system of non-linear transcendental equations that are obtained by forcing the necessary harmonic spectrum [2].

Switching angles in SHEPWM are frequently calculated using the Newton-Raphson method and the theory of elimination by results; however, these approaches mostly depend on a reliable initial estimate, which may result in convergence failures. Conversely, heuristic and evolutionary methods like genetic algorithm, differential evolution (DE), particle swarm optimization, and grey wolf optimization (GWO) are easier to use and less susceptible to this initial approximation. But they run the risk of convergent to local optima too soon, particularly when there are several transcendental equations [9–16]. In [17] authors optimized switching angles for an 11-level PV-fed modular multilevel inverter using GWO and DE independently, demonstrating that GWO produced a lower total harmonic distortion (THD) than DE and enhance output voltage quality.

The **goal** of this study is to investigate the dynamic performance of a wind energy conversion system comprising a grid-connected load, a 13-level hybrid multilevel converter and a DFIG using a PI controller. The study aims to evaluate the dynamic performance and power quality of wind energy conversion systems, and to develop a novel hybrid metaheuristic method combining DE and GWO-based SHEPWM control strategies. This method reduces THD and ensures compliance with IEEE 519 standards, while increasing the power transferred to the grid. The proposed system is shown in Fig. 1 [9–16].

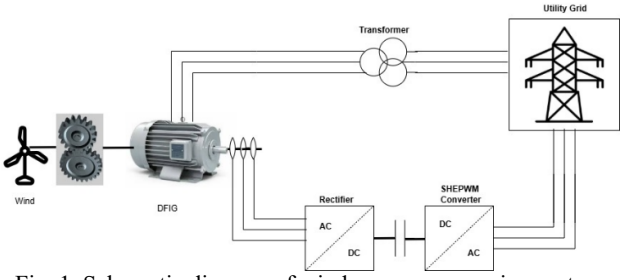

Fig. 1. Schematic diagram of wind energy conversion system

Proposed multilevel converter. Figure 2 shows this topology, which consists of a single complete bridge (A bridge in H) and the cascading of a converter suggested by 7 levels. A switch and 4 diodes make up the auxiliary circuit in the lower H-bridge, which is positioned between 2 DC sources [15].

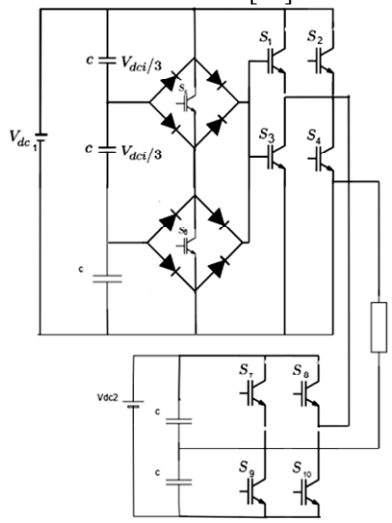

Fig. 2. The proposed 13-level hybrid converter

To generate stepped output voltages, the 13-level hybrid converter combines a diode-clamped (neutral-point clamped, NPC) stage with a cascaded H-bridge. The NPC leg generates levels of 0, $\pm V_{dc}/3$, $\pm 2V_{dc}/3$, and $\pm V_{dc}$, while the H-bridge adds 0 or $\pm V_{dc}$. By summing both outputs, the converter achieves 13 voltage levels from $-V_{dc}$ to $+V_{dc}$ in $V_{dc}/6$ increments, resulting in increased waveform quality with fewer switches and lower THD [12].

To determine the number of levels N of this inverter, the following formula will be applied by adopting a rating per unit *p.u.*:

$$N = 2(3V_{dc1} + 1V_{dc2}) + 1; \tag{1}$$

$$V_{dc1} = 1\,p.u.; \quad V_{dc2} = 3\,p.u. \tag{2}$$

This indicates that in order to get 13 voltage levels, the voltage source linked to the 2nd cell must be 4 times bigger than the single voltage source utilized in the 1st cell [5, 10, 11]. Table 1 presents the appropriate switching states corresponding to each feasible combination.

Table 1

Switching logic of a 13-level hybrid converter

Levels	Output voltage	S_1–S_6 state	S_7–S_{10} state
6	$+V_{dc}$	S_1,S_3 ON	all OFF
5	$+5V_{dc}/6$	S_1,S_3 ON	S_7,S_{10} ON
4	$+2V_{dc}/3$	S_1,S_3 ON	all OFF
3	$+V_{dc}/2$	S_1,S_4 ON	S_7,S_{10} ON
2	$+V_{dc}/3$	S_1,S_4 ON	all OFF
1	$+V_{dc}/6$	S_3,S_4 ON	S_7,S_{10} ON
0	0	S_3,S_4 ON	all OFF
–1	$-V_{dc}/6$	S_3,S_4 ON	S_8,S_9 ON
–2	$-V_{dc}/3$	S_2,S_4 ON	all OFF
–3	$-V_{dc}/2$	S_2,S_4 ON	S_8,S_9 ON
–4	$-2V_{dc}/3$	S_2,S_4 ON	all OFF
–5	$-5V_{dc}/6$	S_2,S_4 ON	S_8,S_9 ON
–6	$-V_{dc}$	S_2,S_4 ON	all OFF

Implementation of proposed algorithm. The output phase voltage's Fourier series expansion is expressed as follows [9–12]:

$$V_0(\theta)=\sum_{n=1,3,5,7,..17}^{\infty} b_n \sin(n\theta), \quad (3)$$

where n=1, 3, 5, 7,…17 are the odd harmonics; θ is the switching angle; b_n is given by:

$$b_n=\sum_{n=1,3,5}^{2N-1}\frac{4V_{dc}}{n\pi}V_1\cos\left((n\theta_1)+...+V_m\cos(n\theta_N)\right), \quad (4)$$

where N is the number of switching angles per quarter cycle; n = 1, 3, 5 ... 2N–1 (odd harmonics); m is the number of DC sources.

By solving (4) and determining the best switching angles, the 5th, 7th, 11th, 13th and 17th harmonics are eliminated. The output voltage waveform's quality is determined by how many harmonics it contains [11, 12].

The main goal of the SHEPWM technique is to determine the firing angles (θ_1 – θ_6) that satisfy the fundamental at the required level V_0 for each modulation index. It also has the advantage of suppressing or eliminating undesirable lower order harmonics from the output phase voltage. The SHEPWM technique has the superior ability and control to eliminate undesirable lower order non-triple harmonics from the output of PWM. The quarter waveform's switching angles must adhere to the following restriction in order to guarantee a symmetrical and physically accurate quarter waveform [13, 14].

$$\theta_1<\theta_2<\theta_3<\theta_4<\theta_5<\theta_6<\pi/2. \quad (5)$$

An objective function is then needed for the optimization procedure, which is selected to gauge how well the selected harmonic rank is eliminated while maintaining the fundamental element at a predetermined value. Consequently, the following is the representation of this objective function [12, 14, 15]:

$$F(\theta)=\sum_{i=1}^{p=6}\cos(\theta_i-\pi M_i)^2+\sum_{i=5,7,11}V_i^2; \quad (6)$$
$$M_i=\pi V_1/5V_{dc},$$

where M_i is the modulation index; V_i is the contribution of the harmonic of order i in the waveform. It can be defined as V_1 fundamental voltage divided by V_{dc} total number of DC component voltage as shown in (6).

Using the suggested algorithm DE-GWO, optimal switching angles are found by minimizing equation (6) under constraint (5).

Overview of GWO technique. In order to identify global maxima and minima for optimization issues, swarm intelligence algorithms mathematically model the hunting habits of animals and birds. One of the swarm intelligence algorithms is the GWO algorithm [18]. In essence, the grey wolves serve as the model for the GWO algorithm. Because they live in packs and have strong social dominance structure, grey wolves are the top predators in the food chain. Figure 3 shows the social order of grey wolves and the 3rd best option [15, 16].

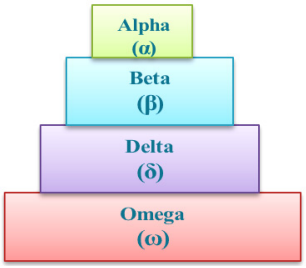

Fig. 3. Social hierarchy of grey wolves

When hunting, grey wolves can encircle their victims and capture them in packs. In order to quantitatively model the encircling behavior, in [15, 17, 18] was proposed the following equations:

$$D=\left|CX_p(t)-X(t)\right|; \quad (7)$$

$$X_p(t+1)=X_p(t+1)-AD, \quad (8)$$

where t is the t^{th} iteration; A, C, D are the coefficient vectors; X_p depicts the prey's location vector; X is the grey wolf's position vector.

The following equation can be used to evaluate the vectors A and C

$$A=2ar_1-a; \quad (9)$$

$$C=2r_2, \quad (10)$$

where r_1, r_2 are the random vectors in [0, 1]; a is the vector that decrease from 2 to 0 as we decrease the number of iteration and it can be calculated as:

$$a=2-2t/t_{\max}, \quad (11)$$

where t and $t_{\max}$ are the current iteration and maximum number of iterations respectively.

The wolf (solution) veers off course and looks in a different direction: if $|A|>1$ and move in the direction of the target (optimal solution), if $|A|<1$, and A is a random vector in the interval [−2a, 2a] where a decreases from 2 to 0 over the course of iteration. When the value of C is greater than one, the C vector often favors exploration, and when the value of C is less than one, it favors exploitation. C is not linearly decreased in contrast to A, therefore, especially in the last iteration, this parameter is quite helpful in preventing the stalling of local optima [17, 18].

The three best optimal solutions are alpha α, beta β and delta δ solutions. The remaining omega ω solutions update their position based on the positions of alpha, beta and delta. The following equations describe how the omega solutions update their position. Grey wolves are able to memorize the position of prey, and because alpha wolves are the leaders in the peck, they have the most knowledge of prey [15]:

$$D_\alpha=\left|C_1X_\alpha-X\right|; \quad (12)$$

$$X_1=X_\alpha-A_1D_\alpha; \quad (13)$$

$$D_\beta=\left|C_2X_\beta-X\right|; \quad (14)$$

$$X_2=X_\beta-A_2D_\beta; \quad (15)$$

$$D_\delta=\left|C_3X_\delta-X\right|; \quad (16)$$

$$X_3=X_\delta-A_3D_\delta; \quad (17)$$

$$X(t+1)=(X_1+X_2+X_3)/3, \quad (18)$$

where X_α, X_β, X_δ are the positions of α, β, δ, respectively; t is the number of iterations; A_1-A_3 are the random vectors [17].

Despite its performance for large-scale problems, the GWO still experiences difficulties with small-scale problems such as the one discussed here (only 2 dimensions), which can cause it to get stuck in local minima. To solve this problem, the DE algorithm is introduced; it adds randomness and improves the ability to escape local minima. However, DE converges rather slowly. In order to achieve better overall performance, a new approach called DE-GWO is proposed. It combines the advantages of both methods by merging GWO (with a better convergence factor) and DE (with a dynamic scaling factor). A target vector representing the population is initialized randomly [10].

Detailed steps of hybrid DE-GWO.

Step 1. Initialization. Create random possible switching angles inside Eq. (5): 6 switching angles [θ_1–θ_6], population size N_p=30 wolves.

Step 2. Evaluate fitness function. Reduce THD while removing certain harmonics (5th, 7th, 11th, 13th, 17th) and maintaining the fundamental voltage magnitude.

Step 3. Determine the alpha α, beta β and delta δ wolves. Evaluate the fitness of the wolves (solutions).

Step 4. Update on GWO position (hunting & encircling) using (12) – (18).

Step 5. DE hybridization by avoiding local optima, mutation and crossover enhances exploration.

Mutation expressed by the following equation:

$$V_i = X_{r1} + F\left(X_{r2} - X_{r3}\right), \tag{19}$$

where V_i is the mutant vector; F is the mutation factor (F= 0.5); $r_1 - r_3$ are coefficients which selected randomly.

Crossover. Using probability crossover rate CR, combine the parent and mutant by the following equation:

$$U_i(j) = \begin{cases} V_i(j), & \text{if rand} < CR; \\ X_i(j), & \text{otherwise}, \end{cases} \tag{20}$$

where U_i is the test vector; X_i is the parent vector; CR is the crossover rate (CR=0.9).

Selection. The best solution (reduced THD) should be kept.

Step 6. Assessment of the new population. For every wolf, recalculate the THD and harmonic restrictions and refresh alpha α, beta β and delta δ.

Step 7. Stopping until fitness convergence or maximum iterations.

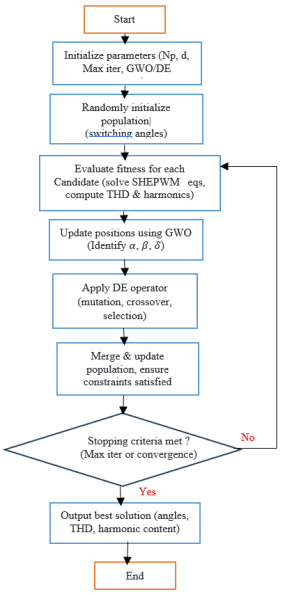

Fig. 4. Flowchart of DE-GWO

DE-GWO process used to determine the ideal firing angles for SHEPWM is shown in Fig. 4 [10].

The optimal switching angles (in degrees) versus modulation index are shown in Fig. 5 while the angles are computed with a fine step-size of 0.01 which corresponds to:

$\theta_1 = 6.2832°$,
$\theta_2 = 18.4642°$,
$\theta_3 = 31.5773°$,
$\theta_4 = 44.7139°$,
$\theta_5 = 57.0695°$,
$\theta_6 = 68.8813°$.

Figure 6 illustrates the dependence on modulation index corresponding to the amplitude of odd number harmonics of 5th, 7th, 11th, 13th and 17th order.

Results indicate differences in the behaviors according to harmonic orders. At modulation index M_i = 0, 5th and 7th harmonics indicate an exponential decay with the primary starting amplitudes of 0.2 and 0.145. The initial amplitudes are also much smaller (0.05–0.09) and the exponential decrease is not as apparent for the higher harmonics (11th and 17th).

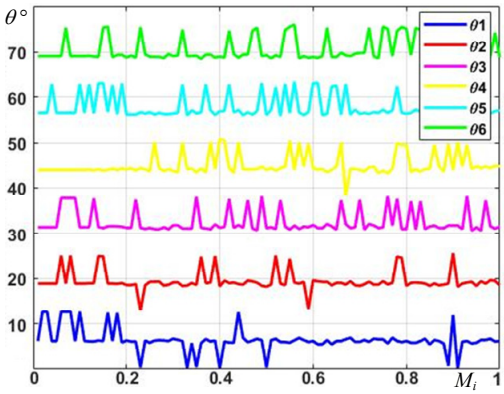

Fig. 5. Switching angles versus modulation index

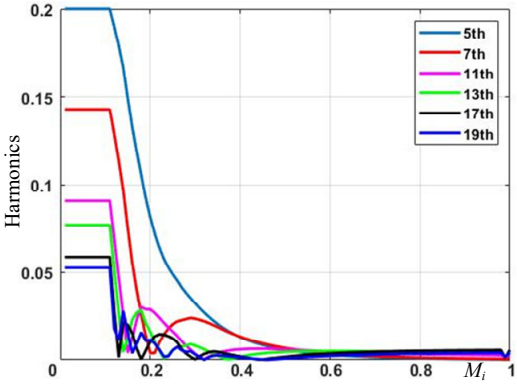

Fig. 6. Harmonics content versus modulation index

Figure 7 shows that the M_i that achieved the lowest percentage of THD was 3.1447 %, and only the lowest THD from the set of angles corresponding to each modular index was chosen.

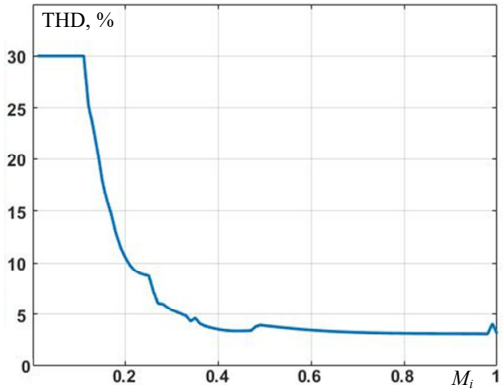

Fig. 7. THD versus modulation index

Turbine modeling. The modeling of a wind energy system is given by [19–22]:

$$\begin{cases} P_v = \dfrac{\rho S v^3}{2}; \; P_{aer} = \dfrac{C_p(\lambda,\beta)\rho S v^3}{2}; \\ T_{aer} = \dfrac{P_{aer}}{\Omega_t} = \dfrac{C_p(\lambda,\beta)\rho S v^3}{2\Omega_t}, \end{cases} \tag{21}$$

where P_v is the mechanical power; P_{aer} is the aerodynamic power; ρ is the air density (1.22 kg/m^3); S is the area of the wind wheel; R is the radius of the blade; Ω_t is the turbine speed; v is the wind speed; T_{aer} is the aerodynamic torque.

The power coefficient C_p depends on the blade tilt angle β and the tip speed ratio λ [20, 21]:

$$\begin{cases} C_p = 0.5176\left(\dfrac{116}{\lambda_i} - 0.4\beta - 5\right)e^{\frac{21}{-\lambda_i}} + 0.0068\cdot\lambda; \\ \lambda_i = \dfrac{1}{\lambda + 0.008\beta} - \dfrac{0.0035}{\beta^3 + 1};\ \lambda = \dfrac{\Omega_t R}{v}. \end{cases} \quad (22)$$

Follow equations are used to simulate the gearbox that connects the turbine to the generator [22]:

$$T_{em} = T_{tur}/G;\quad \Omega_{mech} = G\Omega_t, \quad (23)$$

where T_{em} is the electromagnetic torque; T_{tur} is the turbine torque; G is the ratio's gearbox; Ω_{mech} is the generator's speed.

The fundamental dynamic equation of a mechanical system on a DFIG shaft [20, 22] is:

$$J\frac{d\Omega_{mech}}{dt} + f\Omega_{mech} = T_{mech} - T_{em}, \quad (24)$$

where J is the generator and the turbine moment of inertia; f is the friction coefficient; T_{mech} is the mechanical torque.

Model of DFIG. The following matrix form represents the generator's Park state model [23]:

$$\begin{cases} V_{sd} = R_s i_{sd} + \dfrac{d}{dt}\varphi_{sd} - \omega_s\varphi_{sq}; \\ V_{sq} = R_s i_{sq} + \dfrac{d}{dt}\varphi_{sq} - \omega_s\varphi_{sd}; \end{cases} \quad (25)$$

$$\begin{cases} V_{rd} = R_r i_{rd} + \dfrac{d}{dt}\phi_{rd} - \omega_r\phi_{rq}; \\ V_{rq} = R_r i_{rq} + \dfrac{d}{dt}\phi_{rq} - \omega_r\phi_{rd}, \end{cases} \quad (26)$$

where R_s, R_r are the stator and rotor phase resistances; φ_{sd}, φ_{sq} are d-q components of the stator and rotor flux; V_{sd}, V_{sq} are d-q components of the stator voltage; V_{rd}, V_{rq} are d-q components of the rotor voltage; $\omega_s = \omega_r + \omega$; ω_s, ω_r are the angular frequencies of stator and rotor currents; $\omega = p\,\Omega_{mec}$ is the electrical speed; p is the number of pairs of poles.

The stator and rotor fluxes are:

$$\begin{cases} \phi_{sd} = L_s i_{sd} + M i_{rd}; \\ \phi_{sq} = L_s i_{sq} + M i_{rq}; \end{cases} \quad (27)$$

$$\begin{cases} \phi_{rd} = L_r i_{rd} + M i_{sd}; \\ \phi_{rq} = L_r i_{rq} + M i_{sq}, \end{cases} \quad (28)$$

where i_{sd}, i_{sq}, i_{rd}, i_{rq} are d-q components of the stator and rotor currents; L_s, L_r, M are the stator, rotor and mutual inductances.

The DFIG's electromagnetic torque T_{em} and stator active P_s and reactive power Q_s are expressed as [23]:

$$\begin{cases} P_s = V_{sd} i_{sd} + V_{sq} i_{sq}; \\ Q_s = V_{sq} i_{sq} - V_{sd} i_{sq}; \end{cases} \quad (29)$$

$$T_{em} = \frac{3}{2} p \frac{M}{L_s}(\phi_{sq} i_{rd} - \phi_{sd} i_{rq}). \quad (30)$$

The development of equations that relate the values of the rotor voltages generated by an inverter to the stator active and reactive power will enable the independent control of active and reactive power, hence facilitating the control of wind-generated electricity [23, 24]. With the stator's flux assumed to be constant, we get:

$$\begin{cases} V_{sd} = 0; \\ V_{sq} = V_s; \end{cases} \quad (31)$$

$$\begin{cases} P_s = V_s i_{sq}; \\ Q_s = V_s i_{sd}. \end{cases} \quad (32)$$

The stator and rotor currents are:

$$\begin{cases} i_{sd} = -\dfrac{M}{L_s} i_{rd} + \dfrac{\phi_s}{L_s}; \\ i_{sq} = -\dfrac{M}{L_s} i_{rq}. \end{cases} \quad (33)$$

We replace the currents in (32) by (33) to get the expression of powers in function of stator currents:

$$\begin{cases} P_s = -V_s \dfrac{M}{L_s} i_{rq}; \\ Q_s = \dfrac{V_s^2}{L_s\omega_s} - \dfrac{V_s M}{L_s} i_{rd}. \end{cases} \quad (34)$$

We must determine the relationship between the rotor current and voltages in order to properly manage the machine [22–25]:

$$\begin{cases} V_{rd} = R_r i_{rd} + \left(L_r - \dfrac{M^2}{L_s}\right)\dfrac{di_{rd}}{dt} - g\omega_s\left(L_r - \dfrac{M^2}{L_s}\right) i_{rq}; \\ V_{rq} = R_r i_{rq} + \left(L_r - \dfrac{M^2}{L_s}\right)\dfrac{di_{rq}}{dt} - g\omega_s\left(L_r - \dfrac{M^2}{L_s}\right) i_{rd} + g\dfrac{V_s M}{L_s}, \end{cases} \quad (35)$$

where g is the asynchronous machine's slip.

Indirect field-oriented control of the DFIG. Using the dynamic equations, a template-based PI regulator is built to guarantee steady operation and enable independent control of the DFIG's active and reactive power.

The principle of control by stator field direction is to orient the stator field along the axis d, that is to say:

$$\begin{cases} \phi_{sd} = \phi_s; \\ \phi_{sq} = 0. \end{cases} \quad (36)$$

Figure 8 shows a control scheme of DFIG [19, 20, 25, 26].

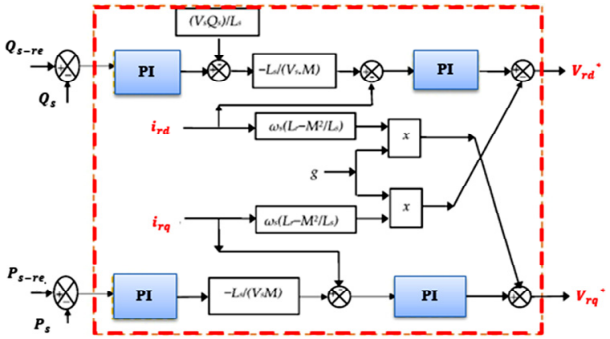

Fig. 8. Control scheme of DFIG

Simulation results. The control scheme proposed in this study aims at controlling the rotor-side of the wind energy conversion system composed of a DFIG, 13-level multilevel converter and connected load. The system was simulated in MATLAB/Simulink at a steady wind speed of 12 m/s, relating to moderate to high operational conditions. Figures 9–19 show the transient and steady state response of the system.

Figure 9 shows that the power is maximal at 2.5 MW and it increases with the wind speed up to the threshold,

reached at 12 m/s, and then remains constantly. This demonstrates the multilevel converter regulates the power applied to the load to avoid overload after the rated power. The coefficient C_p increases till an optimal wind velocity is reached (6.12 m/s) and then decreases, which means that the wind turbine is most efficient at that speed.

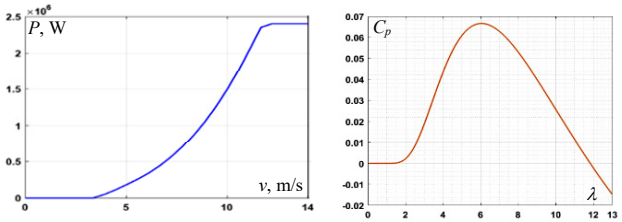

Fig. 9. Power of turbine according to wind speed

Figure 10 displays the shaft's mechanical speed for DFIG. A stable and controlled generator system is shown by the DFIG's shaft mechanisms, which rapidly accelerate from rest to nominal operation speed and then operate at steady, constant speeds.

Figure 11 shows the DFIG torque as a function of time. DFIG initially oscillates with enormous torque for a short period before quickly stabilizing. This demonstrates the damping and smooth operation of the generator after a period of disturbance.

The 3-phase stator currents of the DFIG are shown in Fig. 12. In the first few moments, the currents show strong oscillations and irregularities. These oscillations soon disappear, and the currents stabilize in the form of regular, balanced sinusoids, indicating stable, normal operation of the DFIG.

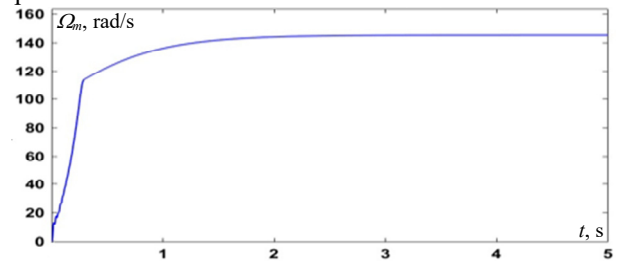

Fig.10. Mechanical speed of the shaft

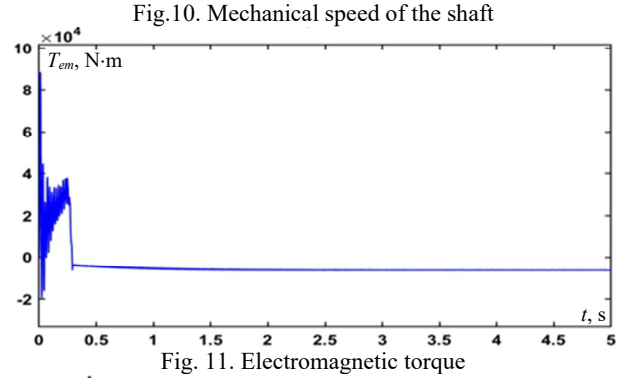

Fig. 11. Electromagnetic torque

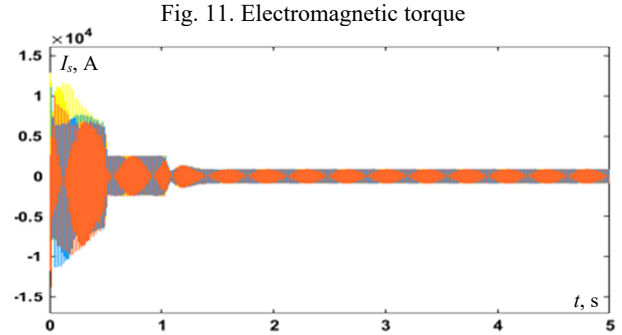

Fig. 12. 3-phase stator currents

The FFT of the 3-phase stator currents of the DFIG is shown in Fig. 13. Regarding the FFT analysis, 3-phase stator currents of the DFIG is mostly sinusoidal (THD = 1.19 %) satisfactory power quality with effective control of the generator.

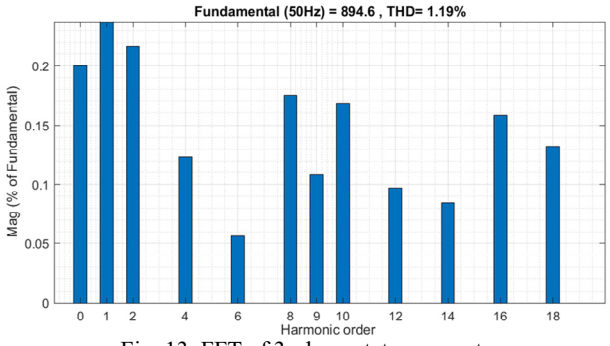

Fig. 13. FFT of 3-phase stator currents

The 3-phase rotor currents i_r of a DFIG is shown in Fig. 14 as a function of time from 0 to 5 s. The rotor currents show noticeable oscillations and irregularities at (t = 0), indicating a transient response to machine start-up. The machine operates smoothly and efficiently when the oscillations cease rapidly and the currents stabilize in balanced, sinusoidal and symmetrical waveforms.

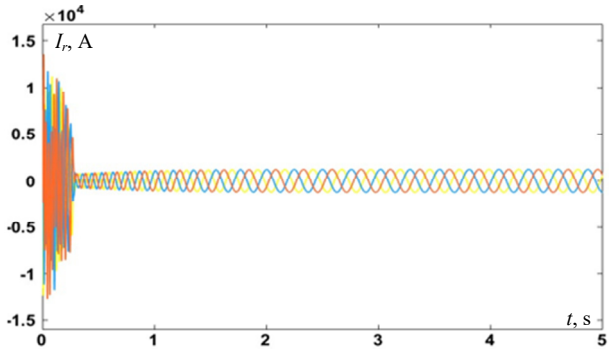

Fig. 14. 3-phase rotor currents

Figure 15 shows the FFT of the 3-phase rotor currents of a DFIG. This FFT analysis shows that the 3-phase rotor currents of the DFIG is predominantly sinusoidal, with a low level of THD = 3.24 %. This indicates effective current control and good power quality in the rotor circuit.

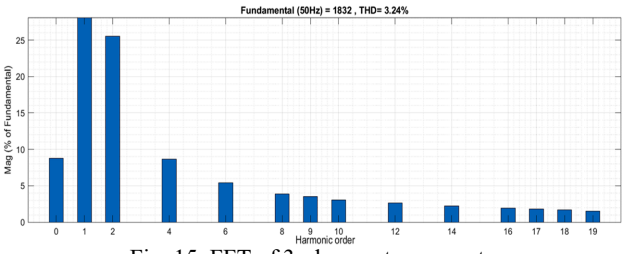

Fig. 15. FFT of 3-phase rotor currents

Figure 16 shows the 3-phase stator voltages over a period of 5 s. These voltages have a symmetrical sinusoidal waveform with amplitude of ±563.38 V, indicating balanced 3-phase operation. There are no visible distortions or irregularities, suggesting stable and normal operation of the generator. Figure 17 shows the zoom of the stator phase voltages.

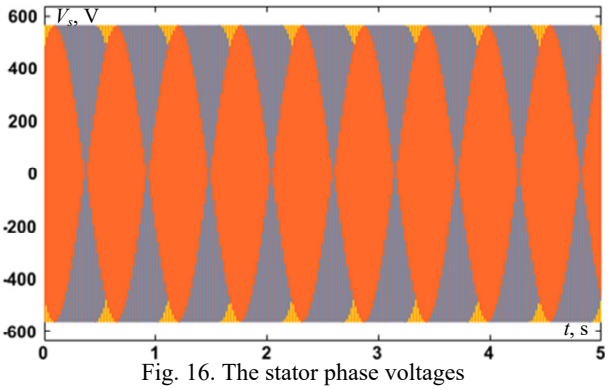

Fig. 16. The stator phase voltages

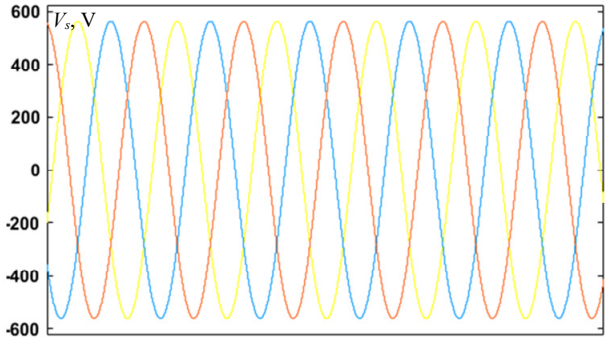

Fig. 17. Zoom of the stator phase voltages

Figure 18 shows the harmonic spectrum of the stator phase voltages, with the magnitude of each harmonic order expressed as a percentage of the fundamental component. THD is 4.18 %, which is relatively low, indicating that the stator phase voltage is predominantly sinusoidal with minor harmonic distortion.

Figure 19 shows the active power response of a load provided by a system that consists of a DFIG and a multilevel converter. Following an initial, highly oscillatory transient, the active power rapidly stabilizes to zero, exhibiting robust damping and a stable steady-state.

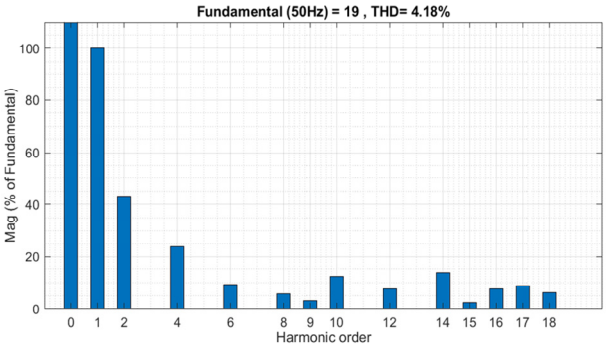

Fig. 18. FFT of the stator phase voltages

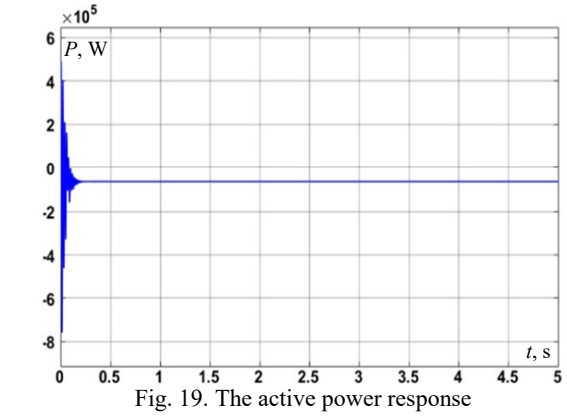

Fig. 19. The active power response

Conclusions. The results of this study demonstrate that the dynamic performance and power quality of grid-connected wind energy systems are greatly enhanced by combining a DFIG controlled by PI controller with a 13-level multilevel converter, which is optimized using a hybrid GWO and DE algorithm for SHEPWM.

The suggested method successfully reduces low-order harmonics and keeps THD within IEEE 519 standards where the 3-phase stator-current THD is 1.19 %, well below the IEEE 519 limit; the stator phase-voltage THD is 4.18 %, and the rotor-current THD is 3.24 %, as shown by MATLAB/Simulink simulations.

The converter topology ensures effective energy transfer and improves the quality of the voltage waveform, confirming the potential of intelligent optimization techniques and hybrid multilevel converters to advance high-performance wind energy applications. These findings offer important new information for creating reliable and effective renewable energy systems that work with contemporary power grids.

Conflict of interest. The authors declare that they have no conflicts of interest.

REFERENCES

1. Tamalouzt S., Benyahia N., Rekioua T., Rekioua D., Abdessemed R. Performances analysis of WT-DFIG with PV and fuel cell hybrid power sources system associated with hydrogen storage hybrid energy system. *International Journal of Hydrogen Energy*, 2016, vol. 41, no. 45, pp. 21006-21021. doi: https://doi.org/10.1016/j.ijhydene.2016.06.163.

2. Shihabudheen K.V., Pillai G.N., Krishnama Raju S. Neuro-Fuzzy Control of DFIG Wind Energy System with Distribution Network. *Electric Power Components and Systems*, 2018, vol. 46, no. 13, pp. 1416-1431. doi: https://doi.org/10.1080/15325008.2018.1499154.

3. Jaladi K.K., Sandhu K.S. Real-time simulator based hybrid controller of DFIG-WES during grid faults design and analysis. *International Journal of Electrical Power & Energy Systems*, 2020, vol. 116, art. no. 105545. doi: https://doi.org/10.1016/j.ijepes.2019.105545.

4. Hafaiedh H., Saoudi Y., Benamor A., Chrifi–Alaoui L. Wind farms integration into power system with improved location and stability problem solving. *Electrical Engineering & Electromechanics*, 2025, no. 5, pp. 10-16. doi: https://doi.org/10.20998/2074-272X.2025.5.02.

5. Parimalasundar E., Jayanthi R., Suresh K., Sindhuja R. Investigation of efficient multilevel inverter for photovoltaic energy system and electric vehicle applications. *Electrical Engineering & Electromechanics*, 2023, no. 4, pp. 47-51. doi: https://doi.org/10.20998/2074-272X.2023.4.07.

6. Gianto R. Steady-state model of DFIG-based wind power plant for load flow analysis. *IET Renewable Power Generation*, 2021, vol. 15, no. 8, pp. 1724-1735. doi: https://doi.org/10.1049/rpg2.12141.

7. Li S., Li L. Steady-state Solution and Evaluation Indices of DFIG Operating at Synchronous Speed (sDFIG). *2021 IEEE Sustainable Power and Energy Conference (ISPEC)*, 2021, pp. 260-267. doi: https://doi.org/10.1109/iSPEC53008.2021.9736024.

8. Tamalouzt S., Belkhier Y., Sahri Y., Bajaj M., Ullah N., Chowdhury M.S., Titseesang T., Techato K. Enhanced Direct Reactive Power Control-Based Multi-Level Inverter for DFIG Wind System under Variable Speeds. *Sustainability*, 2021, vol. 13, no. 16, art. no. 9060. doi: https://doi.org/10.3390/su13169060.

9. Padmanaban S., Dhanamjayulu C., Khan B. Artificial Neural Network and Newton Raphson (ANN-NR) Algorithm Based Selective Harmonic Elimination in Cascaded Multilevel Inverter

for PV Applications. *IEEE Access*, 2021, vol. 9, pp. 75058-75070. doi: https://doi.org/10.1109/ACCESS.2021.3081460.
10. Sifat Z., Hussain M.T., Khan M.A., Hussain M.S., Sarwar A., Tariq M., Hasan M. Selective harmonic elimination in PUC-5 multilevel inverter using hybrid IGWO-DE algorithm. *Engineering Reports*, 2024, vol. 6, no. 10, art. no. e12883. doi: https://doi.org/10.1002/eng2.12883.
11. Dahidah M.S.A., Konstantinou G., Agelidis V.G. A Review of Multilevel Selective Harmonic Elimination PWM: Formulations, Solving Algorithms, Implementation and Applications. *IEEE Transactions on Power Electronics*, 2015, vol. 30, no. 8, pp. 4091-4106. doi: https://doi.org/10.1109/TPEL.2014.2355226.
12. Bektas E., Karaca H. GA Based Selective Harmonic Elimination for Multilevel Inverter with Reduced Number of Switches: An Experimental Study. *Elektronika Ir Elektrotechnika*, 2019, vol. 25, no. 3, pp. 10-17. doi: https://doi.org/10.5755/j01.eie.25.3.23670.
13. Kumar S.S., Iruthayarajan M.W., Sivakumar T. Evolutionary algorithm based selective harmonic elimination for three-phase cascaded H-bridge multilevel inverters with optimized input sources. *Journal of Power Electronics*, 2020, vol. 20, no. 5, pp. 1172-1183. doi: https://doi.org/10.1007/s43236-020-00112-9.
14. Kala P., Arora S. Implementation of PSO based Selective Harmonic Elimination Technique in Multilevel Inverters. *2018 2nd IEEE International Conference on Power Electronics, Intelligent Control and Energy Systems (ICPEICES)*, 2018, pp. 605-610. doi: https://doi.org/10.1109/ICPEICES.2018.8897309.
15. Ceylan O., Neshat M., Mirjalili S. Cascaded H-bridge multilevel inverters optimization using adaptive grey wolf optimizer with local search. *Electrical Engineering*, 2024, vol. 106, no. 2, pp. 1765-1779. doi: https://doi.org/10.1007/s00202-021-01441-z.
16. Nasser A.M., Refky A., Shatla H., Abdel-hamed A.M. A grey wolf optimization-based modified SPWM control scheme for a three-phase half bridge cascaded multilevel inverter. *Scientific Reports*, 2024, vol. 14, no. 1, art. no. 7016. doi: https://doi.org/10.1038/s41598-024-57262-0.
17. Stonier A.A., Chinnaraj G., Kannan R., Mani G. Investigation and validation of an eleven level symmetric modular multilevel inverter using grey wolf optimization and differential evolution control algorithm for solar PV applications. *Circuit World*, 2020, vol. 47, no. 1, pp. 117-127. doi: https://doi.org/10.1108/CW-12-2019-0197.
18. Mirjalili S., Mirjalili S.M., Lewis A. Grey Wolf Optimizer. *Advances in Engineering Software*, 2014, vol. 69, pp. 46-61. doi: https://doi.org/10.1016/j.advengsoft.2013.12.007.
19. Djebbar M.S., Boukadoum A., Bouguerne A. Performances of a wind power system based on the doubly fed induction generator controlled by a multi-level inverter. *International Journal of Power Electronics and Drive Systems (IJPEDS)*, 2023, vol. 14, no. 1, pp. 100-110. doi: https://doi.org/10.11591/ijpeds.v14.i1.pp100-110.
20. Sayeh K.F., Tamalouzt S., Sahri Y. Improvement of power quality in WT-DFIG systems using novel direct power control based on fuzzy logic control under randomness conditions. *International Journal of Modelling and Simulation*, 2025, vol. 45, no. 1, pp. 55-67. doi: https://doi.org/10.1080/02286203.2023.2270757.
21. Kaddache M., Drid S., Khemis A., Rahem D., Chrifi-Alaoui L. Maximum power point tracking improvement using type-2 fuzzy controller for wind system based on the double fed induction generator. *Electrical Engineering & Electromechanics*, 2024, no. 2, pp. 61-66. doi: https://doi.org/10.20998/2074-272X.2024.2.09.
22. Kumar Behara R., Kumar Saha A. Deep Q-Network Reinforcement Learning-Based Rotor Side Control System of a Grid Integrated DFIG Wind Energy System Under Variable Wind Speed Conditions. *IEEE Access*, 2024, vol. 12, pp. 184179-184205. doi: https://doi.org/10.1109/ACCESS.2024.3511665.
23. Benbouhenni H., Yessef M., Colak I., Bizon N., Kotb H., AboRas K.M., ELrashidi A. Dynamic performance of rotor-side nonlinear control technique for doubly-fed multi-rotor wind energy based on improved super-twisting algorithms under variable wind speed. *Scientific Reports*, 2024, vol. 14, no. 1, art. no. 5664. doi: https://doi.org/10.1038/s41598-024-55271-7.
24. Muthukaruppasamy S., Dharmaprakash R., Sendilkumar S., Parimalasundar E. Enhancing off-grid wind energy systems with controlled inverter integration for improved power quality. *Electrical Engineering & Electromechanics*, 2024, no. 5, pp. 41-47. doi: https://doi.org/10.20998/2074-272X.2024.5.06.
25. L'Hadj Said M., Ali Moussa M., Bessaad T. Control of an autonomous wind energy conversion system based on doubly fed induction generator supplying a non-linear load. *Electrical Engineering & Electromechanics*, 2025, no. 4, pp. 3-10. doi: https://doi.org/10.20998/2074-272X.2025.4.01.
26. Alnaib I.I., Alsammak A.N. Optimization of fractional PI controller parameters for enhanced induction motor speed control via indirect field-oriented control. *Electrical Engineering & Electromechanics*, 2025, no. 1, pp. 3-7. doi: https://doi.org/10.20998/2074-272X.2025.1.01.

Received 02.09.2025
Accepted 25.12.2025
Published 02.05.2026

R.F. Abdelgoui [1], *Doctor of Technical Science, Associate Professor,*
R. Taleb [2], *Full Professor,*
[1] Laboratory of Industrial Engineering and Sustainable Development (GIDD), Department of Electrical Engineering, Ahmed Zabana University, Algeria,
e-mail: rimfeyrouz.abdelgoui@univ-relizane.dz (Corresponding Author)
[2] Electrical Engineering Department,
Laboratoire Génie Electrique et Energies Renouvelables (LGEER), Hassiba Benbouali University, Algeria.

How to cite this article:
Abdelgoui R.F., Taleb R. Enhanced power quality in grid-connected wind energy systems using PI-controlled with doubly fed induction generator optimized by hybrid differential evolution and grey wolf algorithm. *Electrical Engineering & Electromechanics*, 2026, no. 3, pp. 34-41. doi: https://doi.org/10.20998/2074-272X.2026.3.05